

A Method to Investigate Non-Thermal Effects of Radio Frequency Radiation on Pharmaceuticals with Relevance to RFID Technology

Felicia C.A.I. Cox, Vikas K. Sharma, Alexander M. Klibanov, Bae-Ian Wu *Member, IEEE*,
Jin A. Kong *Fellow, IEEE*, and Daniel W. Engels *Member, IEEE*

Abstract—A method is reported to accurately and precisely control temperature of a solution sample to investigate non-thermal effects of radio frequency radiation (RFR) on pharmaceuticals. This method utilizes a transverse electromagnetic (TEM) cell connected in series with a radiation source. The temperature of a sample under study, within the TEM cell, is regulated using a combination of a fiber-optic thermometer and thermo-electric cooler. It is shown that the sample temperature can be accurately controlled and maintained even under conditions where the RFR can increase the sample temperature via thermal mode. This methodology provides a well-controlled approach to investigate the non-thermal effects of RFR for a range of incident power intensities and frequencies and initial sample temperatures.

I. INTRODUCTION

IN its February 2004 report, the U.S. Food and Drug Administration (FDA) listed Radio Frequency Identification (RFID) technology as an important tool to combat counterfeiting of pharmaceutical products [1]. This technology utilizes labeling of pharmaceutical products with tags, which can be tracked using electromagnetic radiation in the radio frequency range (electromagnetic radiation in the frequency range of 3 KHz – 300 GHz) similar to those used in radio communications, wireless data networks and mobile phones. One of the concerns regarding successful implementation of this technology, however, is whether the RFR is capable of causing deleterious reactions in the drug product leading to reduced potency and/or other undesirable effects.

The effects of RFR on materials have been broadly classified into two categories: thermal effects and non-thermal effects [2]-[4]. **Thermal effects** are defined as

Manuscript received April 3, 2006. This work was supported in part by the HRI/Pharmaceutical Industry Consortium at Auto-ID Labs, Massachusetts Institute of Technology (MIT), Cambridge, MA 02139.

B.-I. Wu is with the Center for Electromagnetic Theory and Applications (CETA) at MIT, Cambridge, MA 02139 USA (phone: 617-253-4028; fax: 617-253-0987; e-mail: biwu@mit.edu).

J. A. Kong is head of CETA at MIT, Cambridge, MA 02139 (e-mail: kong@emwave.org).

F. C. A. I. Cox is with Department of Electrical Engineering at MIT, Cambridge, MA 02139 (e-mail: fcaic@mit.edu).

V. K. Sharma is with Department of Chemistry at MIT, Cambridge, MA 02139 (e-mail: v_sharma@mit.edu).

A. M. Klibanov is with Department of Chemistry and Bioengineering at MIT, Cambridge, MA 02139 (e-mail: Klibanov@mit.edu)

D. W. Engels is with Auto-ID labs at MIT, Cambridge, MA 02139 (e-mail: dragon@csail.mit.edu).

those that stem from an appreciable increase in the temperature of a substance on exposure to RFR, i.e., it is this heating (measurable using an appropriate temperature probe) that is responsible for the observed changes. From the pharmaceutical point of view, it is reasonable to assume that RFR-induced thermal effects would be no different than those induced by conventional bulk heating, for example, as produced by exposing a product to heat in a controlled temperature oven or on the shelf in an uncontrolled room environment. Since the effects of temperature on drug stability are generally well understood, the effects of RFR-induced thermal effects can be easily predicted.

In contrast, **non-thermal effects**, those arising even in the absence of any appreciable increase in the material temperature upon exposure to RFR, are obscure and controversial. Although, there have been a few studies of non-thermal effects of RF radiation on biochemical samples, such as cells and tissues, the conclusions from these studies are inconsistent and provide no mechanistic understanding of the non-thermal effects.

To properly assess the non-thermal effects of RFR, it is important that the temperature of the sample under study is precisely and accurately controlled and maintained. This should be true even under conditions where the RFR used would tend to elevate sample temperature. In the few studies published thus far on evaluating the non-thermal effects of RFR, temperature stability is usually accomplished by using a low frequency RFR that is not absorbed by the sample or a low power intensity of a high frequency RFR such that the temperature increase is not appreciable [5],[6]. The overall temperature control is obtained by keeping the test-assembly in controlled conditions. However, no direct means of temperature control is used to maintain precise sample temperature in these prior studies. This approach limits the use of a high power intensity of a high frequency RFR (e.g., those in the microwave region) since the temperature increase due to absorbed power would be much greater and thermal effects would become important. The reason for using above-mentioned approaches to attain temperature control is presumably due to the fact that materials commonly used for temperature control such as metallic surfaces and liquids, interfere with the absorption of RFR by the sample under consideration.

In this paper we describe a method and apparatus for accurately maintaining sample temperature, while the sample is being exposed to RFR, under conditions, where in the absence of such control, the sample temperature would increase substantially. We show that this methodology and assembly is capable of maintaining the sample temperature within $\pm 0.5^\circ\text{C}$ precision, irrespective of the RFR frequency, intensity, or initial sample temperature. This methodology provides an accurate way to investigate non-thermal effects of RFR on a variety of samples.

II. MATERIALS AND METHODOLOGY

A. General

The test apparatus was composed of five physical subsystems: the test sample subsystem, the radiation exposure (RF exposure) subsystem, the power measurement subsystem, the temperature measurement and control subsystem, and an overall control subsystem. The equipment required for the apparatus is listed in Table 1; Figure 1 provides an equipment connection diagram.

In the following subsections, we describe each of these subsystems.

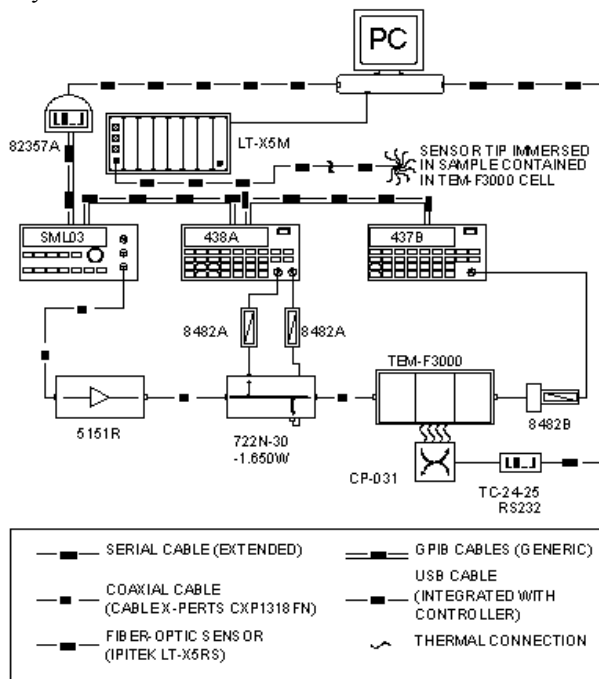


Fig. 1. Equipment connection diagram. Equipment labels shown are model numbers for devices listed in Table 1. (See Table 1)

B. Test sample subsystem

The test chamber was a TEM cell - a wave guide that allows propagation of electromagnetic plane waves in the TEM mode, also called the fundamental or TM_0 mode [7]. As shown in Figure 2, the cell (Montena TEM-F3000) was fabricated with a copper plate suspended in the middle of the chamber. This plate was used as a platform for supporting the sample - 1.5mL of aqueous solution in a

standard 1.8mL vial - in a hand-made supporting "bed" of Rohacell, a material which is transparent to radiation at radio and microwave frequencies. The bed ensured that the vial made physical contact with the upper inner surface of the TEM cell and was fixed in place by friction (Figure 3). The septum of each vial was punctured to create a hole about the same size as the temperature sensor (Ipitek Lumitherm LT-X5RS). The sensor was first inserted through a hole in the door of the TEM cell and then through a tiny funnel into the vial. This technique minimized evaporative and leakage losses and sensor damage.

TABLE 1
EQUIPMENT SPECIFICATION

Make and model	Description
Agilent 82357A	USB/GPIB interface for Windows
Cable X-perts CXP1318FN	50 Ohm, low loss, 3ft coaxial cable with "N" male connectors
Dell PC	Computer running MATLAB 7
Hewlett Packard 438A	Dual input power meter with remote capabilities and 5-ft sensor cables
Hewlett Packard 437B	Single input power meter with remote capabilities and 5 ft sensor cables
Hewlett Packard 8482A	100mW coaxial power sensor; range: 1 μ W to 100mW
Hewlett Packard 8482B	25W coaxial power sensor with power dissipation and heat sink; range: 1W to 25W
Ipitek Lumitherm LT-X5R	Fiber optic thermometer processing unit with remote capabilities
Ipitek Lumitherm LT-X5RS	Fiber optic temperature sensor
MECA 722N-30-1.650W	Dual directional coupler; range: 800MHz to 2.5GHz
Montena TEM-F3000	Closed TEM cell for measurements up to 3GHz; 50 Ohm load required
New Brunswick Scientific Company G24	environmental incubator shaker (not shown in Figure 1)
Ophir 5151R	Radio frequency power amplifier, 0.8 - 2.5 GHz, 25Watt
Rohde and Schwarz SML03	9kHz to 3.3GHz signal generator with remote capabilities
TE Technology CP-031	Thermo-electric cooler, -20°C to 100°C. Also known as a peltier cooler.
TE Technology TC-24-25 RS232	Thermo-electric temperature controller and power supply with remote capabilities
TE Technology TP-1	Thermal paste (not shown in Figure 1)
Miscellaneous items	GPIB cables, network cable (RJ45), 12AWG wire (cooler interconnection), serial cable, etc.

With the exception of the miscellaneous cables, all devices listed above are shown in the connection diagram (Fig. 1) using model numbers only.

C. RF exposure subsystem

The signal generator (Rohde & Schwarz SML03), power amplifier (Ophir 5151R), dual directional coupler (MECA 722B-30-1.650W) and TEM cell were connected in series using coaxial cables (Cable X-perts CXP1318FN), satisfying the 50 Ω input/output impedance requirements for several of these devices. Two of the four ports on the coupler and one of the two ports on the TEM cell were used for interconnection while the remaining three ports were used for power measurements.

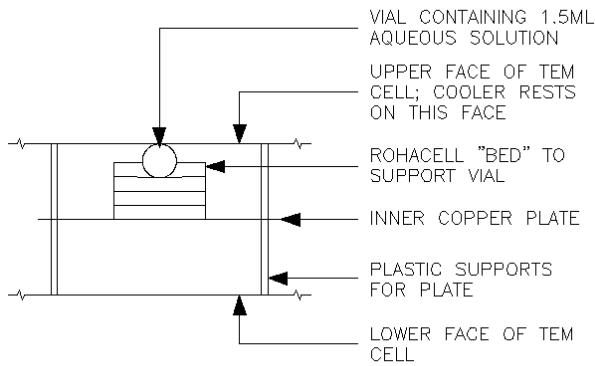


Fig. 2. Partial section through TEM cell, showing vial and supporting "bed"

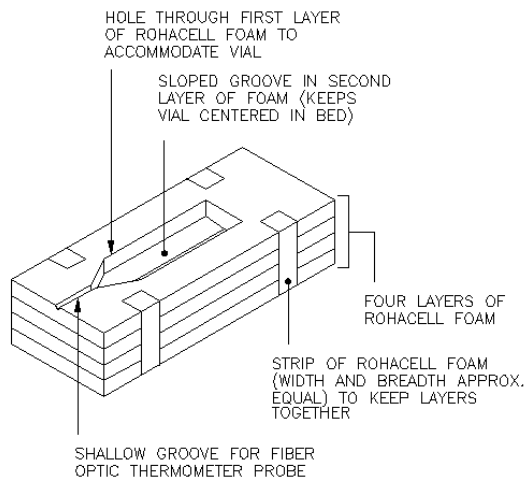


Fig. 3. Rohacell "bed" for supporting sample vials within the TEM cell.

D. Power measurement subsystem

The directional coupler provided a power attenuation of approximately 30dBm between the input and the coupled ports, one sampling the incident power from the power amplifier and the other, the reflected power from the TEM cell. Sensors (Hewlett Packard (HP) 8482A) were connected to each of the coupled ports and to channels A and B of the dual input power meter (HP 438A). A third sensor (HP 8482B) was connected to the output of the TEM cell and to the single channel power meter (HP 437B) in order to measure the transmitted power.

Due to input power constraints for the sensors (Table 1) and gain/attenuation provided by the amplifier and coupler, the control software was designed to avoid damage to physical components by limiting user inputs.

E. Temperature measurement and control subsystem

The test sample subsystem was placed in a controlled temperature oven (New Brunswick Scientific Company G24 environmental incubator shaker) which allowed manual control of the ambient temperature within the TEM cell. Sample temperature was determined using the

fiber optic thermometer (Ipitek Lumitherm LT-X5R): the sensor was connected to port 1 of the thermometer and its tip immersed in the sample, as described in part B.

With the sample vial in contact with the upper inner surface of the TEM cell as indicated in part B, the cooler was positioned above the sample but on the upper external surface of the cell. Thermal paste (TE Technology TP-1) applied to the surface of the cooler improved thermal conductivity. This arrangement maximized heat exchange between the cooler and the sample.

F. Control subsystem

Computer controllable devices were connected to the Dell PC by one of three methods. First, the signal generator and power meters were connected via GPIB cables to the GPIB interface (Agilent 82357A), which was plugged into one of the USB ports on the computer. Second, the thermometer was directly connected via network cable and used TCP/IP for communication. Third, the cooler controller was plugged into the computer's COM1 port via serial cable.

All the devices were manipulated from scripts (programs) in the MATLAB 7 environment, which contained the *visa-gpib*, *serial* and *tcpip* instrument functions necessary for communication. The final program allowed the user to choose one of four exposure conditions: temperature control only, RFR exposure only, both conditions simultaneously or neither. User inputs included incident RFR frequency and power intensity, the required temperature and the exposure duration. The script stored all data in text-based LOG (.log) files and provided a processing option to plot data and perform specific absorption rate (SAR) calculations.

III. EXPERIMENTAL RESULTS AND DISCUSSION

Herein we have developed a procedure and a set-up to accurately and precisely control and maintain temperature of a sample solution when irradiated with RFR. Evaluation of the implemented system required two sets of experiments, the first to show the effects of RFR on sample temperature, and the second to determine whether the system designed could limit such effects. Two different frequencies, 2.45 GHz and 915 MHz were used to evaluate their effects on sample temperature at two different incident radiation power levels of 22W and 4W.

Figure 4 shows the effect of RFR frequency, power intensity and initial sample temperature on time-course of sample temperature in the apparatus described in Part II, and without direct sample cooling. Clearly, an increase in sample temperature was observed in all cases, except for in the case of 915 MHz at 4W incident power and 30°C. The extent of the increase was dependent on the RFR frequency, RFR intensity and initial sample temperature. The maximum increase in sample temperature, $\Delta T \approx 9^\circ\text{C}$, was observed in the case of 2.45 GHz RFR at 22W incident radiation power and initial sample temperature

50°C. The extent and rate of sample temperature increase is reduced by using a lower frequency, power and initial sample temperature.

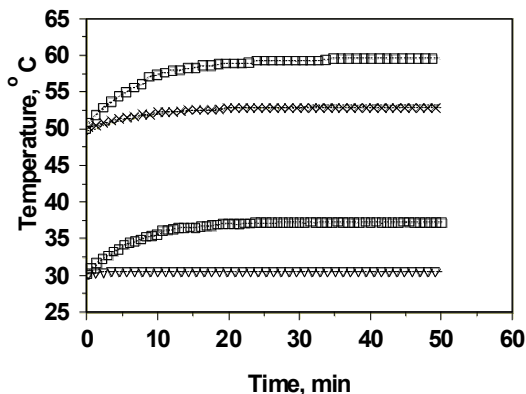


Fig. 4. Effect of the frequency, intensity, and initial sample temperature on the time-course of sample temperature upon exposure to radiofrequency radiation. 2.45 GHz at 22W (open squares), 915 MHz at 22W (open circles), 2.45GHz at 4W (crosses) and 915 MHz at 4W (open triangles). The curve obtained with 2.45 GHz at 4W at initial sample temperature of 50°C overlays that of 915 MHz at 22W at the same initial temperature.

To determine whether the apparatus met the stated goal of maintaining sample temperature regardless of RFR exposure, the performance of the apparatus was evaluated under the harshest conditions investigated in the first set of experiments – 2.45GHz, 22W incident power and 30°C initial temperature.

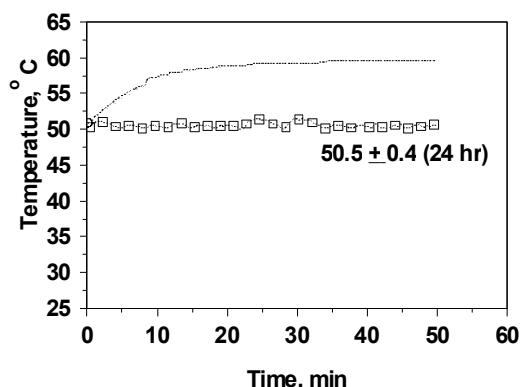


Fig. 5. Effect of the external peltier cooling device on sample temperature upon exposure to radiofrequency radiation at 2.45 GHz and 22W incident power. No external cooling (open circles); with external cooling (Open squares).

Figure 5 compares the time-course of sample temperature as the sample was exposed to the stated conditions without active cooling to that with active cooling. With cooling, the sample temperature stabilized at an average of 50.5°C, with a maximum variation of $\pm 0.4^\circ\text{C}$ for up to 24 hours.

IV. CONCLUSIONS

This study demonstrates that radio-frequency radiation at 915MHz and 2.45GHz increased sample temperatures

but that the assembled system reported here significantly limited RFR induced-heating in aqueous samples. Use of this equipment and its software allows tests with any given RFR/temperature combination. Therefore, the apparatus allows to investigate RFR-induced non-thermal effects (physical/chemical) in aqueous solutions of such pharmaceuticals as drugs and biologics at any RFR frequency, power intensity and sample temperature combination.

ACKNOWLEDGMENT

The authors thank Robin Koh and Tom Scharfeld for their early work in establishing this project. The authors also thank Dennis Kim, Jim Dowden and Tom Pizzuto for their support and encouragement of this work.

REFERENCES

- [1] U.S. Department of Health and Human Services, Food and Drug Administration, Combating Counterfeit Drugs: A Report of the Food and Drug Administration, February 18, 2004. Available: http://www.fda.gov/oc/initiatives/counterfeit/report02_04.html
- [2] J. L. Kirschvink, "Microwave absorption by magnetite: a possible mechanism for coupling nonthermal levels of radiation to biological systems," *Bioelectromagnetics*, vol. 17, pp. 187-194, 1996.
- [3] E. Marani and H. K. P. Feiraband, "Future perspectives in microwave applications in life sciences," *Eur. J. Morphol.*, vol. 32, pp. 330-334, 1994.
- [4] M. Porcelli, G. Cacciapuoti, S. Fusco, R. Massa, G. d'Ambrosio, C. Bertoldo, M. D. Rosa, V. Zappia, "Non-thermal effects of microwaves on proteins: thermophilic enzymes as model system," *FEBS Lett.*, vol. 402, pp. 102-106, 1997.
- [5] D. I. de Pomerai, B. Smith, A. Dawe, K. North, T. Smith, D. B. Archer, I. R. Duce, D. Jones, and E. P. M. Candido, "Microwave radiation can alter protein conformation without bulk heating," *FEBS Lett.*, vol. 543, pp. 93-97, 2003.
- [6] E. Bismuto, F. Mancinelli, G. d'Ambrosio, and R. Massa, "Are the conformational dynamics and the ligand binding properties of myoglobin affected by exposure to microwave radiation?," *Eur. Biophys. J.*, vol. 32, pp. 628-634, 2003.
- [7] J. A. Kong, *Electromagnetic Wave Theory*, EMW Publishing, Cambridge MA, USA.